DEVELOPMENT OF THE STEEL TYPE SEISMIC-ISOLATION DEVICE (METAL LINK BEARING)

Katsuhiro NISHIMURA[1], Kenji IKEDA[2], Hiroshi MITAMURA[3], Akio HAYASHI[4] And TOSHIHIKO BESSHO[5]

SUMMARY

Earthquake proofing bearing supports of a bridge constructed in a cold region should be those which are not affected by temperature change and able to work stably at any temperature throughout the year. To meet this condition, a bearing support with the following structure is developed: a top concave shoe is placed in the upper part as usual and between the top concave shoe and a convex rotator which is attached to the bottom concave, a lens shaped turning board is installed. The turning board whose surface has only controlled microscopic frictional resistance can move freely against horizontal forces and touches the top and bottom concave shoes within the range of the curvature radius R of the convex rotator.

In this equipment, when relative displacement occurs on the top and bottom concave shoes, the turning board rotates along the convex rotator to be lifted by the restoration force that causes the relative displacement. The force lifts the top concave shoe can work to produce restoring force of a bearing support.In addition, energy absorption caused by the controlled microscopic frictional resistance is expected to work for the earthquake proof of the bridge bearing support. Accordingly, a theoretical analysis and a performance test was conducted concerning the geometrical restoration caused by the relative displacement between the top and bottom concave shoes and the energy absorption by the friction of the turning board.

As a result, the experiment in which rigid foundation simulation was conducted acquired the response including the displacement in spite of large friction stress. Also, the decrease of inertia force was recognized.

The test results could be estimated by setting a friction angle for models of mass system and by a time history analysis. The equation to estimate the test result gives safer values because it does not take the decrease that occurs around the part most largely displaces into consideration, so that the estimation could be used as a histeresis curve in design.

In a simple design model, the earthquake proofing bearing support was shown to restrict plastic deformation of a bridge pier.

INTRODUCTION

The South Hyogo Earthquake, which occurred on January 17, 1995, caused serious damage to various structures of the same degree as the Great Kanto Earthquake. It goes without saying that many bridge components were greatly damaged (some bridge piers collapsed and some bridge beams fell).

To protect bridges from such earthquake damage, bridges are designed emphasizing the improvement of aseismatic capabilities. The authors of this paper focused on a seismic-isolation design in which the superstructure is supported by seismic-isolation bearings installed on the substructure. We have designed bearings in consideration of the operation environment and examined the functions of the bearings.

[1]   Civil Engineering Research Institute,Hokkaidou Development Bureau, JAPAN FAX;+81-11-820-2714
[2]   Civil Engineering Research Institute,Hokkaidou Development Bureau, JAPAN FAX;+81-11-820-2714
[3]   Civil Engineering Research Institute,Hokkaidou Development Bureau, JAPAN FAX;+81-11-820-2714
[4]   Pacific Consultanta CO.,LTD.,7-5Sekido.1.Tama-shi,Tokyo 206-0011,JAPAN TEL;+81-042-372-0111
[5]   The Japan Steel Works Co.,Ltd.,4.cattuchou,muroranshi, 051-8505,JAPAN, FAX;+81-143-22-1439

METAL LINK BEARINGS

Operating environment and required performance

Seismic-isolation bearings are usually made primarily of rubber. However, when these bearings are used in cold regions as shown in Fig. 1(type fig), where temperatures fall to -30 in winter, the rigidity increases due to the hardening of the rubber, the hardened rubber loses its functionality when it is placed again at room temperature (15).To ensure the functionality of bearings in such environments, it is necessary to design compact bearings which can be installed in a limited space and ensure stability irrespective of temperature changes.
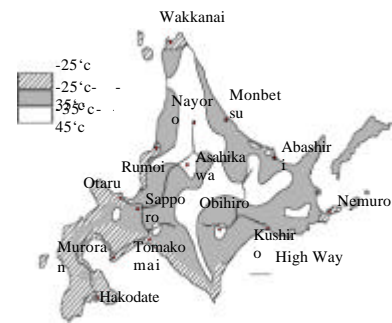
Fig. 1 Minimum temperature distribution in Hokkaido

Structure and characteristics of bearings

Fig 2 (a) shows the structure of a metal link bearing.

The bearing consists of an upper shoe installed on the superstructure, a lower shoe also installed on the substructure, and a rotating plate inserted between these two components. The rotating plate contacts the upper and lower shoes at its curved surface (radius of curvature: R). Thickness (t) is defined as C times the radius of curvature. The dead weight of the superstructure is loaded on the upper shoe as vertical force (V).

Fig2 (b) shows a state in which the upper shoe is pushed right in the fig under the vertical force and relative displacement between the upper and lower shoes is U. In this state, the rotating plate rotates counterclockwise by E to counterbalance the horizontal force (H) pushing the upper shoe. As U increases, the horizontal force (H) increases. The system is therefore elastic. When the horizontal force (H) is suddenly removed, the system will return to the neutral state shown in Fig. 2 (a).
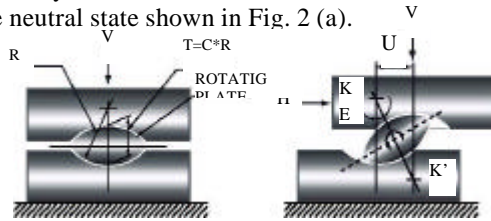
(a) Basic structure (neutral sate)   (b) Displacement conditions

Fig. 2 Operating principle of the metal link bearing   **Fig. 3**
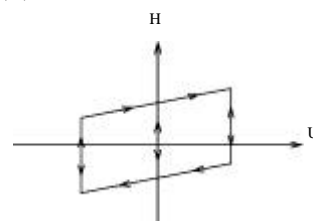
Hysteresis loop

After the maximum displacement (U_B) is determined, relative displacement is periodically tested by pushing the upper shoe right and left. When the vertical force (H) and the relative displacement (U) are plotted, the elastic characteristics shown in Fig. 3 is obtained. The area enclosed by the hysteresis loops is formed because the sliding motions at the contact surface between the rotating plate and the upper / lower shoe are caused by the rotation of the plate due to the relative displacement of the upper and lower shoes. This indicates that friction serves as an important factor in determining the energy absorption capacity of the bearings.

Equations for estimating performance

To incorporate bearing performance into a model, it is necessary to develop equations expressing the bearing performance described in the previous section. As shown in Fig. 2 (b), the relative displacement between the upper and lower bearings occurs due to the linkage in which the center of curvature (point K) of the lower bearing and the center of curvature (point K') of the upper bearing function as levers. The horizontal force (H) can be expressed by Eq. (1), in which additional friction angles (b) are considered.

Hysteresis loops obtained using Eq. (1) are bilinear-type hysteresis loops as shown in Fig. 3.

$$H=V*\tan(E+b) \qquad \text{Eq. (1)}$$

: when the upper shoe moves right

: when the upper shoe moves left

The relationship between U and E is expressed by Eq. (2).

$$U=R*(2-C)*\sin E \qquad \text{Eq. (2)}$$

where the additional friction angle (b) represents the sliding friction occurring between the rotating plate and the upper / lower shoe and functions as a factor which changes based on the friction caused by the upper and lower shoes in accordance with the shape factor (C). When the upper / lower shoe and the rotating plate contact each other on the plane surface, the friction coefficient is represented by f. Equation 3 is a relational expression based on several assumptions regarding the distribution of bearing acting on the rotating plate.

$$\sin b =2f*(1+f^2)^{1/2}/(2-C) \qquad \text{Eq. (3)}$$

Equations (1) to (3) indicate that as R increases and C decreases, the bearing becomes less rigid ; as C decreases, attenuation also decreases. Appropriate selection of these values therefore enables researchers to design bearings which are flexible and have excellent in energy absorption capabilities.

Verification of the equation for estimating performance

To verify Eq. (1), which shows the performance of metal link bearings, FEM analysis was conducted.

Two calculation models (C = 0.2, 0.6) were used under the following conditions: radius of curvature (R) = 300 mm; plane friction coefficient (f)= 0.10; vertical load (V) = 1,960 kN. Fig 4 shows a comparison of FEM analysis results and the equation. In both cases, the equation almost agreed with the analysis results. The equation is therefore believed to be sufficiently accurate.

(a) Shape factor C = 0.2   (b) Shape factor C = 0.6
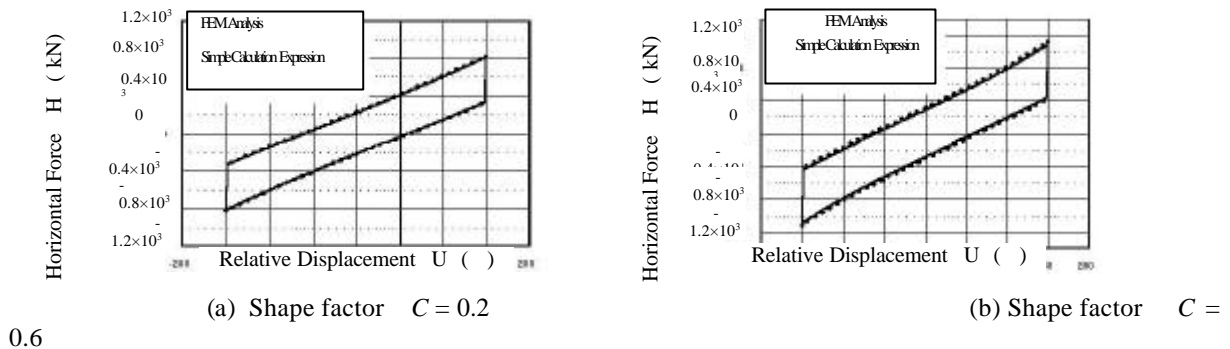
Fig. 4 Comparison of FEM analysis results and the equation

Selection of materials for sliding surfaces

Sliding surfaces require comparatively large loading capacities to support the superstructure in a compact manner as well as friction conditions under which sliding surfaces can move in response to the horizontal load expected to act on the surfaces. As a combination of materials which meet these requirements, PTFE (polytetraflouroethylene) and stainless steel, which are proven materials in Japan, were selected. Friction performance was confirmed through a sliding test. The sliding test was conducted under the following conditions: ±75 mm stroke, sine wave, 0.5 Hz frequency, 20 test temperature. Fig 5 is a schematic diagram of the test equipment, while Photo 1 shows specimens..
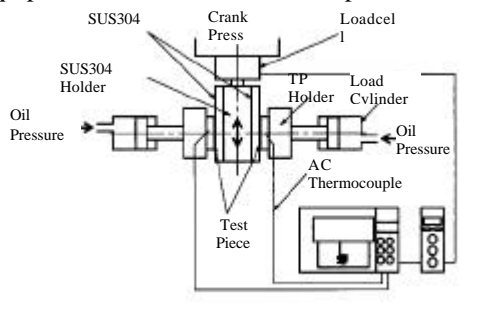
Fig. 5 Schematic diagram of the test equipment (sliding test)   **Photo 1 Specimens**

Table 1 Physical properties of PTFE materials and the results of the sliding test

Test item	Specific weight (25)	Tensile strength (kgf/cm^2)	Elongation (%)	Melting point ( )	Sliding test results (mean friction coefficient) (f)		
					Bearing conditions		
					60 kgf/cm^2	145 kgf/cm^2	290 kgf/cm^2
Measured values	2.20	2.4	280	327	0.125	0.116	0.100

Table 1 shows the physical properties of PTFE materials containing fillers and the results of a sliding test.

No major changes in the mean friction coefficient due to changes in the bearing surface were observed in the range of 60-290 kgf/cm². Particularly when the bearing is expected to be near the allowable compressive stress, the average friction coefficient of 0.1 may be used disregarding any changes in the friction coefficient .

An additional test was conducted under the following conditions: 290 kgf/cm² bearing condition; 0.3 and 0.7 Hz vibration frequencies. The test showed that the mean friction coefficient changed by only approximately 5% and little velocity dependence was observed.

3. VERIFICATION BY VIBRATION TEST

3.1 Preliminary response test

It was clarified that the basic performance of steel link bearings can be expressed by Eq. (1). To determine whether the anticipated response behaviors occurred for structures supported by steel link bearings, the test equipment shown in Fig. 6 was produced for a response test. The test was conducted using roller bearings which can move toward the direction of the vibrations and steel link bearings (R = 250 mm, C = 0.6). The former were installed on two of four fulcrums on the superstructure and the latter were installed on the remaining two fulcrums. The superstructure was supported by these bearings on a vibrating table. The table was vibrated by an electric motor which generated sine waves. The aforementioned test was conducted for three cases of vibration amplitudes of 30 and 60 mm. Frequencies were changed by inverter control at pitches of 0.2 Hz in the range of 1.0-2.0 Hz.
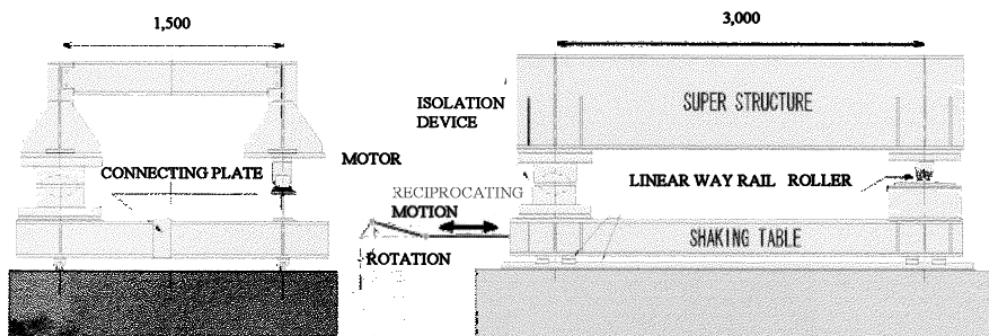
Fig 7 indicates response ratios. These ratios together with displacement response ratios and acceleration response ratios indicate a vibration reduction effect in response to frequency increases. Highly consistent test results and calculation values were also observed. It is therefore believed that the actual behavior of metal link bearings can be estimated by Eq.1.

(a) Displacement response ratios

(b) Acceleration response ratios
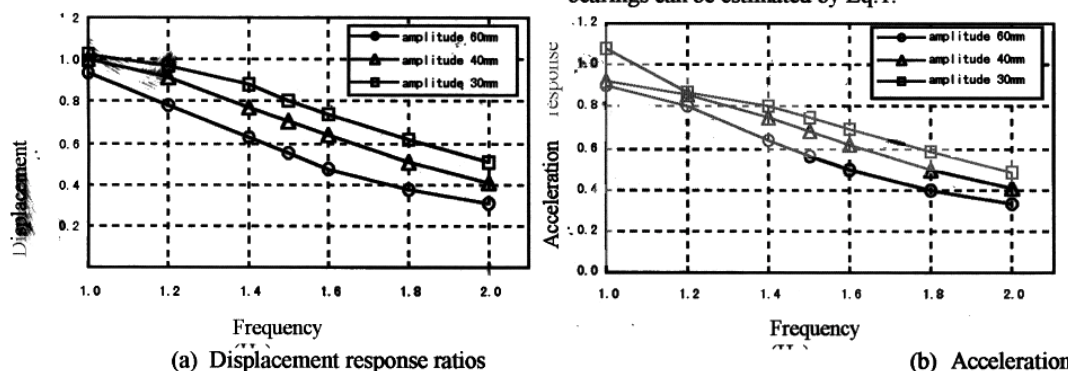
Fig. 7 Response ratios

3.1 Random wave vibration test

The aforementioned preliminary response test changed to a random wave vibration test. In this test, the vibrating table was vibrated not by an electric motor which generated sine waves, but by an actuator which generated random waves. This was done for the following reasons. Actual earthquake motions have various complex characteristics and cannot be completely simulated using only simple continuous wave forms and waves with large amplitude in a 0.5-1.0 cycle. It is also necessary to understand transient vibrations which occur when the structure corresponds to changes in the amplitudes and cycles of input.

waves with large amplitude in a 0.5-1.0 cycle. It is also necessary to understand transient vibrations which occur when the structure corresponds to changes in the amplitudes and cycles of input.

Fig 8 is a conceptual diagram of test equipment. The same superstructure and vibrating table used for the preliminary response test were also used for this test. The movement of an actuator (±1,960 kN dynamic load; ±15 cm stroke) was amplified threefold by a lever which vibrates the vibrating table. A weight of 2,000 kg was added as extra load on the superstructure.

As in the case of the preliminary response test, metal link bearings were installed on two fulcrums on one end of the superstructure and roller bearings were installed on the remaining fulcrums on the other end.
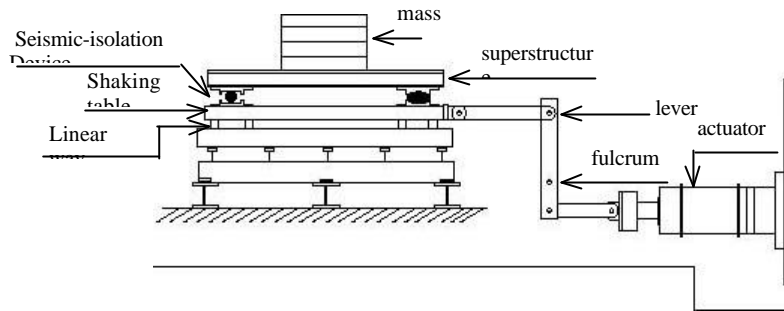
Fig. 8 Conceptual diagram of the test equipment (Random vibration test)

Vibration wave forms generated by actuators have the four wave forms specified below. Figs 9 to 10 show the results of vibration wave forms specified below in (1)-(2). Test results for all cases show that the velocity of the superstructure was lower than that of the vibrating table, demonstrating the effects of metal link bearings.

(1) Pink noise x 2 (wave forms which have specific vibration components in the range of 0.5-10.0 Hz were normalized to twofold amplitudes)

(2) Kobe Marine Meteorological Observation (NS component of wave forms measured at the Kobe Marine Meteorological Observatory during the South Hyogo Earthquake on January 17, 1995)

To simulate behavior during vibrations, calculations were performed using the following two methods: nonlinear time history analysis using wave forms in (1), in which bearing performance is regarded as a bilinear model in Eq. 1; equivalent linear time history analysis using equivalent rigidity and equivalent attenuation constants. The results of these methods are shown in Figs. 11 and 12, respectively.

In the aforementioned analyses, the acceleration time history of the vibrating table is regarded as an input and a model of one material point and one degree of freedom, which consists of mass equivalent to the superstructure and metal link bearings, was used. The plane friction coefficient (f) was 0.1. To correct the differences between the analysis results and test results, the equations for analysis contained viscosity coefficient terms.
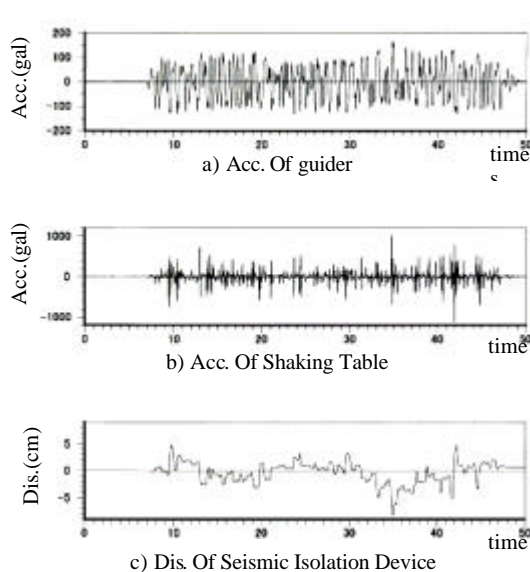
Fig. 9 Pink noise x 2 (test results)
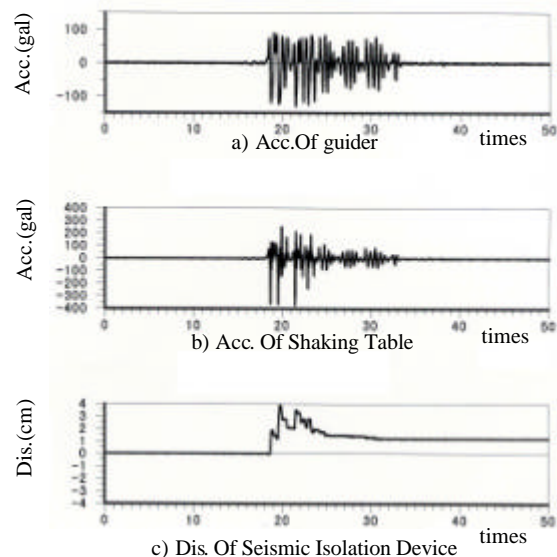
Fig. 10 Kobe Marine Meteorological

Observatory (test results)

(a) Acc. Of Girder Time(s)

(b) Dis. Of seismic Isolatin Device Time(s)

(c) Histeresis Curve Dis.(cm)

(d) Acc.-Dis. Dis.(cm)
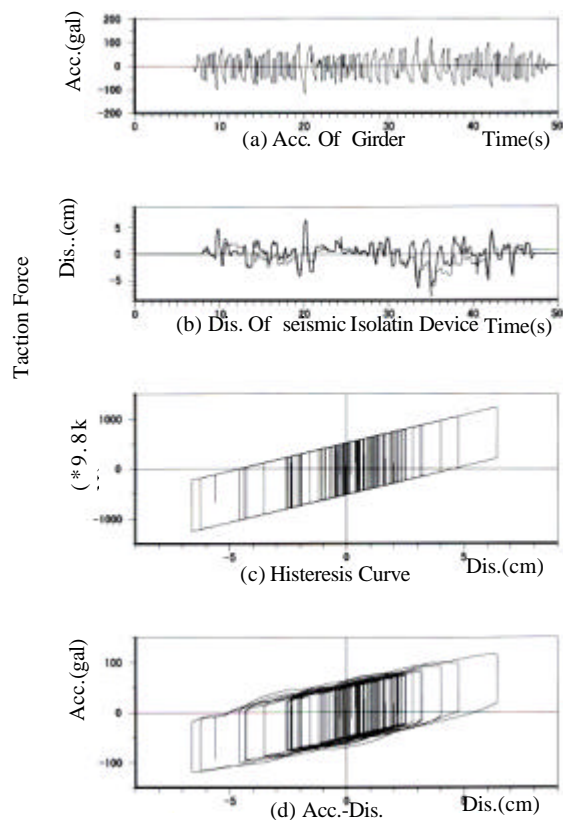
Fig. 11 Results of nonlinear time history analysis

(a) Acc. Of Girder Time(s)

(b) Dis. Of seismic Isolatin Device Time(s)

(c) Hysteresis Curve Dis.(cm)

(d) Acc.-Dis. Dis.(cm)
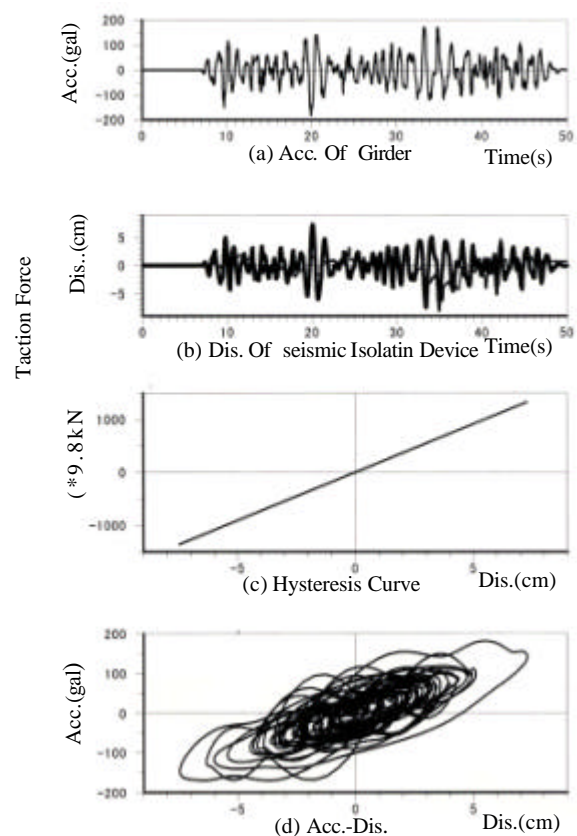
Fig. 12 Results of Equivalent linear time history analysis

The displacement response values of the superstructure in the equivalent linear analysis are slightly larger than the test result and non linear analysis values. This functions as a conservative factor in designing structures. In other words, the attenuation performance of equipment, such as this type of bearing, which have hystereris loops shaped like rectangles is higher than estimates based on the assumed equivalent linear.

Dis.(cm)

Fig.13 Hysteresis loop (test

Fig 13 is a hysteresis loop of bearings whichwere tested using the wave forms in (1). A comparison of the hysteresis loop and that in Fig. 11 shows that the former is a much better simulation. The viscosity coefficient used for this analysis was very small (49 N•s/cm).

TEST USING LARGE DESTRUCTION TEST EQUIPMENT

Large destruction test equipment

After the South Hyogo Earthquake, Japan's aseismic design standards were revised to take into consideration the motions of inland earthquakes represented by the South Hyogo Earthquake with a magnitude of 7 on the Richter scale. Although these earthquakes may not occur, they will greatly affect structures if they do. As shown in Fig. 14, L2 type I earthquake motions are added to the standards.

To verify the safety of bridges, it is necessary to confirm the adequacy of design calculations. Confirmation can be obtained through tests using equipment which can precisely simulate earthquake motions. When the scale of the equipment is closer to the actual scale of the structure to be constructed, higher accuracy can be obtained. With regard to the aforementioned types of structures, which may be hit by hard, repeated earthquake motions during a short period of time, it is believed that free vibration components of the structures are not so large. This is also indicated by the push-over analysis and the energy conservation law. The authors of this paper therefore think that full-scale tests are required. However, when currently available vibrating tables are used, the tables must have a very large capacity. We therefore felt it would be difficult to use conventional vibrating tables and

decided to develop our own original equipment. Fig 15shows the general view of the equipment which consists of a frame (substructure) floating on air bearings, a full-scale bridge specimen installed on the frame and a reaction force wall which causes the frame to collide with the specimen.
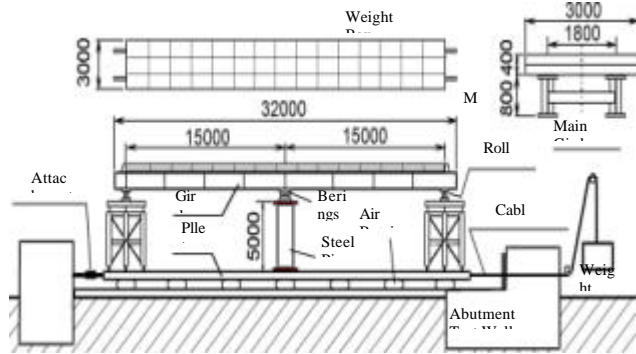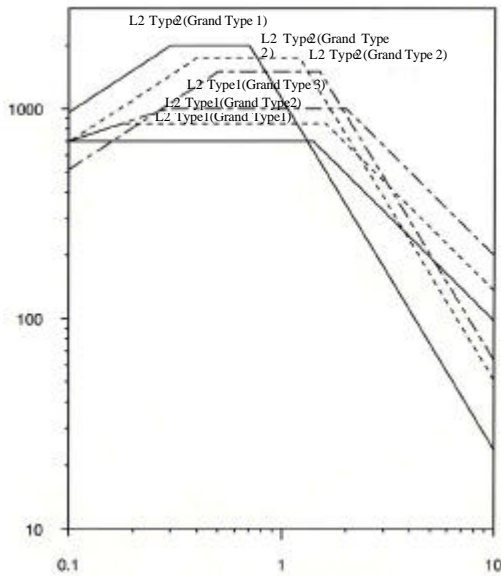
Fig. 15 General view of the test equipment

Test method

As the superstructure of the full-scale bridge specimen, a two-span continuous girder bridge was used (two 15.0 m spans; two H type steel main girders; 1.8 m main girder span; 104.6-ton mass). The fulcrums at the both ends of the girder were supported with two movable rollers and the fulcrums on the middle of the girder were supported with bearings on the two steel pipe bridge piers (ö813 mm outer diameter; 19 mm plate thickness). The test was conducted on two cases to confirm the effects of the bearings. In one case, pin bearings were used for the bearing portion; in the other case, metal link bearings shown in Fig. 16 were used for the bearing portions.

In the test, loading was implemented by having the frame (substructure) attached to the bridge pier collide with the reaction force wall. This was done by using the acceleration force of a free-falling 10-ton weight. In this process, input acceleration acting on the frame was adjusted by changing the travel distance of the frame and the thickness of the buffers (polystyrene foam material).

Fig. 16 Metal link bearings

4.3 Test results

Fig 17 shows an example of input and response acceleration wave forms through a comparison of pin bearings and metal link bearings. In cases in which pin bearings were used, the upper end of the bridge pier had almost the same acceleration wave forms as the superstructure, and the maximum value was 10% larger than the input acceleration. Meanwhile, in cases in which metal link bearings were used, the acceleration of the superstructure was much lower than that of the input acceleration, and vibrations after the collision were also controlled.
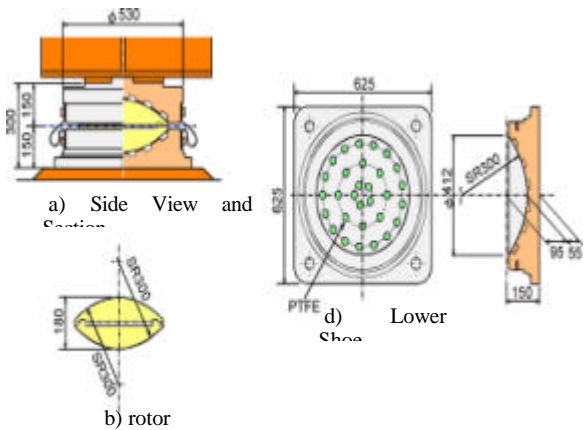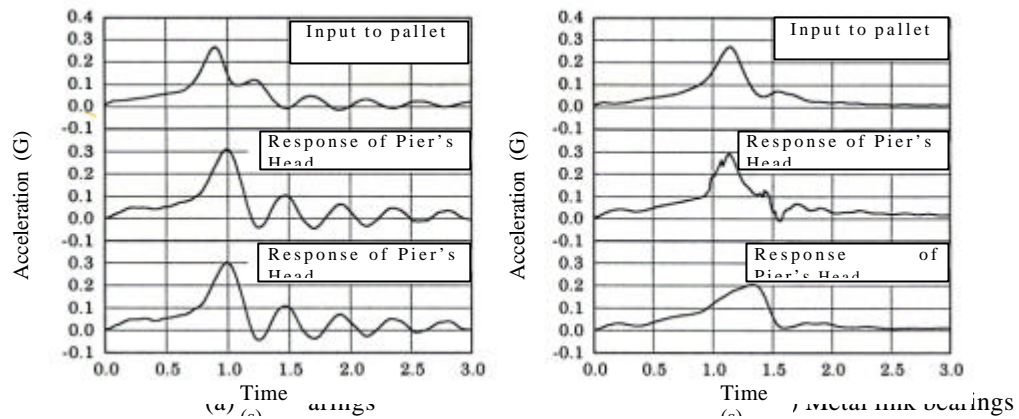
Fig. 17 Acceleration wave forms

CONCLUSION

To put metal link bearings to practical use and incorporate them in the design of structures, the authors of this paper clarified the principles of metal link bearing design and developed equations for their use. Formulation was relatively easy and the correlation of the equations with another method (FEM analysis) was high, indicating that the equations are appropriate. Two-plane friction on the upper and lower surfaces of the rotating plate changes according to the shape factor (C). Outlying singular points are infinite ($C = 2$) and $f / (\quad f^2)^{1/2}$ ($C = 0$). Therefore, the shape factor can be selected in this range.

The results of response tests were highly correlated with the results of simulation calculations, confirming the safety of bearing performance. This was also true in terms of random wave form vibration.

In a full-scale impact inertial loading test, the response acceleration of the superstructure using this type of bearing was approximately 30% lower than that of the superstructure using pin bearings, confirming the superiority of the former.

The bearings operated smoothly and stably during all the tests without reductions in their performance.

Even when temperatures change, this type of bearings continues to function smoothly. This is an important characteristic of these bearings. It is therefore believed that the bearings are very useful in developing seismic-isolation designs for bridges to be constructed in cold regions. We hope that this type of bearing will be frequently used by conducting basic performance tests and developing equations to express the performance of the bearings